

AVANCÉES EN PHYSIQUE DES PARTICULES :
LA CONTRIBUTION DU LEP

ADVANCES IN PARTICLE PHYSICS: THE LEP CONTRIBUTION

High spatial resolution detectors and particle lifetime measurements at LEP

Paschal Coyle^{a*}, Olivier Schneider^b

^a Centre de physique des particules de Marseille, Université de la Méditerranée, 13288 Marseille, France

^b Institut de physique des hautes énergies, Université de Lausanne, CH-1015 Lausanne, Switzerland

Received 15 May 2002; accepted 1 July 2002

Note presented by Guy Laval.

Abstract The design and performance of the LEP silicon vertex detectors are described. Their application to the measurement of the τ -lepton and b-hadron lifetimes is discussed and the current status of these measurements is reviewed. *To cite this article: P. Coyle, O. Schneider, C. R. Physique 3 (2002) 1143–1154.*

© 2002 Académie des sciences/Éditions scientifiques et médicales Elsevier SAS

vertex detectors / silicon / lifetime / b hadrons / tau leptons

Détecteurs à haute résolution spatiale et mesures de la durée de vie des particules à LEP

Résumé La configuration et les performances des détecteurs de vertex au silicium construits à LEP sont décrites. Leur utilisation pour la détermination de la durée de vie du lepton τ et des hadrons b est discutée, et la situation actuelle pour ce type de mesures est passée en revue.

Pour citer cet article : P. Coyle, O. Schneider, C. R. Physique 3 (2002) 1143–1154.

© 2002 Académie des sciences/Éditions scientifiques et médicales Elsevier SAS

détecteurs de vertex / silicium / durée de vie / hadrons b / leptons tau

1. Introduction

In 1983, a very surprising discovery [1] was made with the PEP collider at SLAC: prompt leptons produced in high-energy e^+e^- collisions and assumed to originate from the semi-leptonic decays of b quarks were found to have a mean impact parameter (with respect to the interaction point) corresponding to a b-quark lifetime of $\tau_b \sim 1$ ps, of the same order as that of the c (charm) quark. This was contrary to the expectation $\tau_b \ll \tau_c$, based on the fact that the semi-leptonic decay width of a heavy quark (like c or b) should scale like the fifth power of its mass. The observation of the ‘long’ b lifetime thus implied that the weak interaction couplings (i.e., CKM matrix elements; see the contribution by Kluit and Stocchi [2])

* Corresponding author.

E-mail addresses: Coyle@c ppm.in2p3.fr (P. Coyle); Olivier.Schneider@iphe.unil.ch (O. Schneider).

at work in b decays are much smaller than the ones governing the decays of quarks from the first two generations. This was one of the first insights into the peculiar structure of the CKM matrix, and today's precise measurements of the average b-hadron lifetime are used, together with the inclusive semi-leptonic branching ratios for $b \rightarrow c\ell\nu$ and $b \rightarrow u\ell\nu$, to extract some of the most precise estimates of the CKM matrix elements $|V_{cb}|$ and $|V_{ub}|$.

Another important consequence of this discovery is the possibility of identifying experimentally b-quark decays based on vertex topology, exploiting the measurable spatial separation between the b-decay vertex and the primary interaction vertex. At LEP, the average distance L between these vertices was foreseen to be of the order of a couple millimetres, since $L = (p/m)t$, where m is the mass of the hadron containing the b quark ($\sim 5 \text{ GeV}/c^2$), p its momentum (typically $30 \text{ GeV}/c$ at $\sqrt{s} = m_Z$) and t its proper decay time (of the order of a picosecond). This implied that silicon vertex detectors placed around the LEP beam pipe would certainly provide the necessary spatial resolution to identify the high-energy b-quark jets resulting from the decay of the particles that LEP was supposed to study. Not all LEP experiments had, since the beginning, set the highest priority for building performant vertex detectors. However, their necessity soon became obvious, and each experiment eventually built one, or even upgraded their first version for improved performance.

Something that was perhaps not foreseen at the start of LEP was the importance that heavy flavour physics was going to play in the LEP physics programme, thanks to the use of vertex detectors. Indeed, these detectors were not only used for 'b tagging', but also for detailed studies of b-hadron decays and properties. Altogether, the four LEP experiments collected approximately four million $Z \rightarrow b\bar{b}$ decays, a sample which allowed the opening of a new era in b-hadron physics, and go far beyond what had already been achieved by experiments dedicated to B physics at symmetric e^+e^- machines running at the $\Upsilon(4S)$ resonance. Operating on the Z resonance has two main advantages: all species of b hadrons can in principle be studied (including for example B_s^0 mesons and b baryons which are too heavy to be produced in $\Upsilon(4S)$ decays), and these b hadrons have a large boost (which for example eases vertexing techniques). In addition, the environment is much cleaner than in high-energy hadronic collisions, such as the Tevatron $p\bar{p}$ collider at Fermilab.

In this report, we first describe the design and performance of the vertex detectors built and operated by the LEP collaborations. We then review the lifetime measurements performed at LEP, as examples of the achievements that were made possible with these devices. Others such achievements, discussed elsewhere in this volume, include the first observation (and then accurate measurements) of the time dependence of $B^0-\bar{B}^0$ mixing, high sensitivity searches for $B_s^0-\bar{B}_s^0$ oscillations, precision electroweak studies with $Z \rightarrow b\bar{b}$ decays, and Higgs boson searches in the $b\bar{b}$ mode. A beautiful example of the use of a vertex detector for b tagging and decay length measurement is displayed in Fig. 1.

2. Vertex detectors

The basic principle of a silicon detector is illustrated in Fig. 2. A plate of high purity n-type silicon ($\rho \sim 10 \text{ k}\Omega\cdot\text{cm}$) has strips of p^+ on one side and a layer of highly doped n^+ silicon on the other. The p^+ layer serves to reverse polarise the junction, and the n^+ to prevent the depletion zone from reaching the back plane. Finally, a passivation oxide layer is needed to protect the silicon surface. The passage of a charged particle through the silicon releases electron-hole pairs (3.6 eV needed per pair) which are rapidly collected on the electrodes, their image charge inducing a detectable pulse in the external electronics. Capacitive charge division between the strips allows the interpolation of the particle position between strips and permits a readout pitch larger than the intrinsic strip pitch.

The development of double-sided readout, in which the n^+ layer is also segmented, thereby allowing orthogonal coordinates to be read out from the same single piece of silicon was pioneered at LEP. The advantages are a reduced amount of material and the possibility to perform pulse height correlation between the signals of both coordinates, thus facilitating coordinate matching in the presence of many tracks. In practice, the implementation of double-sided readout was problematic, as a positive fixed oxide charge,

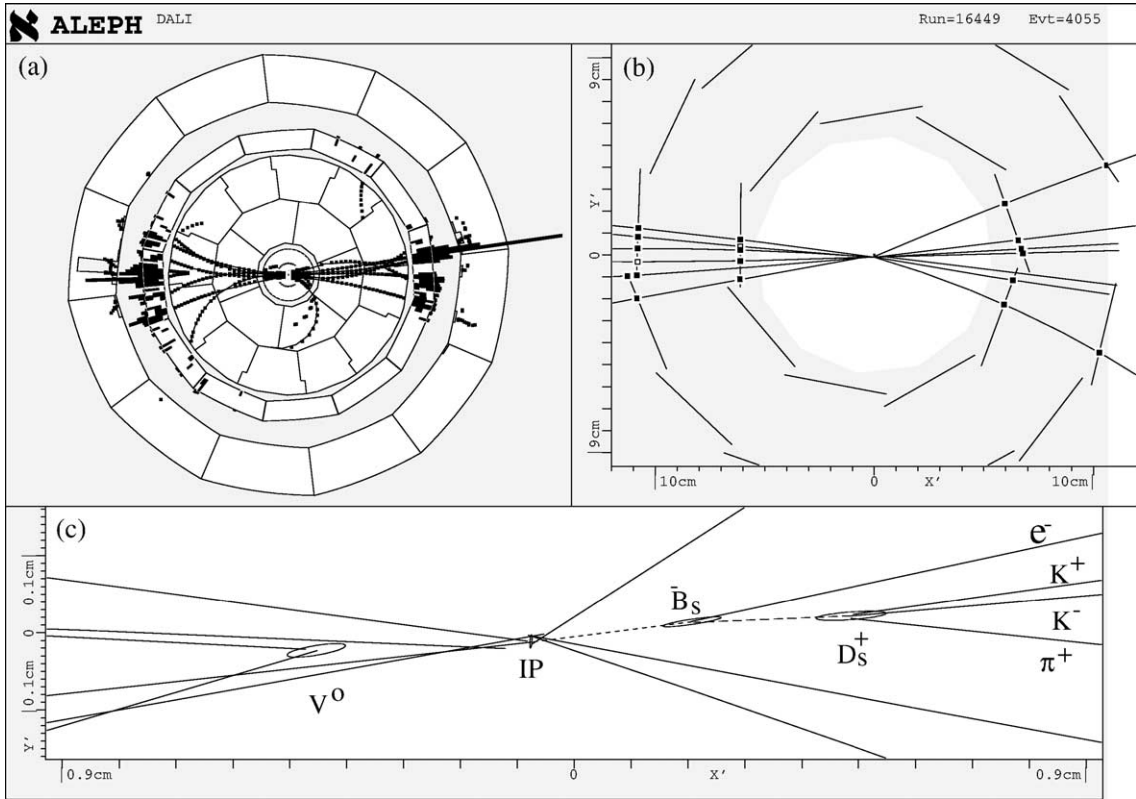


Figure 1. Display of a two-jet event recorded by the ALEPH detector, in which a B_s^0 candidate has been reconstructed in the following mode: $\bar{B}_s^0 \rightarrow D_s^+ e^- \bar{\nu}_e$, $D_s^+ \rightarrow \phi \pi^+$, $\phi \rightarrow K^+ K^-$. (a) Overall view in the plane transverse to the beams; (b) detailed view of the vertex detector, showing the hits in the two layers of silicon; (c) zoom close to the interaction point (IP), showing the reconstructed tracks and vertexes.

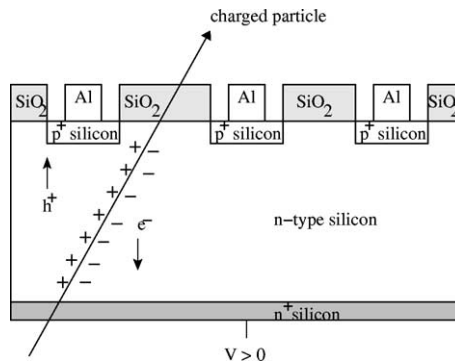


Figure 2. Principle of operation of a silicon particle detector.

inevitably introduced during the passivation step of the detector production, was found to attract electrons forming a conductive layer at the Si–SiO₂ interface which short-circuited any n⁺ strips. Nevertheless, solutions were found: the ALEPH approach was to introduce p⁺ blocking strips between the n⁺ strips, while DELPHI introduced field plates over the oxide to create a field which repelled the electrons.

2.1. Some design considerations

For a system of two detection layers at distances r_1 and r_2 from the interaction point, with corresponding intrinsic spatial resolutions of σ_1 and σ_2 , the resolution on the impact parameter, the closest distance between the track and the primary vertex (see Fig. 6), can be approximated by $\sigma_{\text{ip}}^2 = \sigma_{\text{geom}}^2 + \sigma_{\text{mcs}}^2/p^2$. The first term is the geometrical extrapolation uncertainty

$$\sigma_{\text{geom}}^2 = \left(\frac{\sigma_1 r_2}{r_2 - r_1} \right)^2 + \left(\frac{\sigma_2 r_1}{r_2 - r_1} \right)^2$$

and the second term is determined by the sum of multiple Coulomb scatters of the particle in any elements before the last measurement. The precision on the impact parameter is therefore optimised by making:

- (i) the intrinsic spatial resolution of the sensors as small as possible;
- (ii) the first measurement as close as possible to the interaction point;
- (iii) the lever arm $r_2 - r_1$ as large as possible; and
- (iv) the material of the detector as thin as possible, especially that in front of the first measurement (i.e., the beam pipe).

These four requirements have driven the designs of the LEP vertex detectors.

In order to reduce the multiple Coulomb scattering term, thin detectors ($\sim 300 \mu\text{m}$) were adopted by all experiments. The correspondingly small signal size ($\sim 22\text{k}$ electron–hole pairs) required low-noise pre-amplifiers with large gain. The small diffusion width within the silicon, $\sim 15\text{--}20 \mu\text{m}$ implied a strip pitch of $15\text{--}25 \mu\text{m}$ in order to preserve the intrinsic sensor precision. A corresponding readout pitch of $25\text{--}100 \mu\text{m}$ required the density of the readout electronics to be rather high. The resulting large number of readout channels necessitated multiplexing of the serial readout at a relatively fast frequency. Consequently, it was necessary to develop custom designed very large-scale integrated (VLSI) application specific integrated circuits (ASICs). The fact that the silicon was only available in 4-inch wafer forced the sensors to be daisy chained into faces to achieve the necessary large solid angle coverage, and required large numbers of automated wire bonds to be performed.

In order to reduce the amount of material in the sensitive region, the readout electronics for the strips running perpendicular to the beam direction (z), were located at the end of the faces. This required the development of low mass fanouts (e.g., kapton, glass, polyamide), or extra layers in the sensors themselves, which connected the strips to the electronics.

The extreme spatial precision provided by the detectors also implied stringent constraints on the mechanical aspects of the designs. Very stable, low mass, carbon fibre or beryllium mechanical supports were developed to maintain the position of the faces. To ensure full azimuthal coverage, and also to facilitate alignment of the detector, the mechanical support usually introduced a small overlap between adjacent faces. In order to allow installation of the detector, the mechanical support comprised two separate hemispheres, which were joined together to form a cylinder around the beam pipe. The radius of the LEP beryllium beam pipe (8.5 cm in 1989 and 5.5 cm from 1991) dictated the minimum radius of the innermost layer (~ 6 cm). One or two additional concentric layers were incorporated in the available space between the first layer and the start of the gaseous inner tracking chamber.

Another important issue was the cooling of the readout electronics. A typical readout channel required $\sim 1\text{--}2$ mW of power, implying a total power dissipation of $\sim 100\text{--}200$ W for a full detector of $\sim 100\text{k}$ channels. This heat had to be efficiently removed in order to keep thermal distortions of the mechanical support to acceptable levels, maintain the required mean time between failure of the readout electronics, and reduce thermal effects induced in the neighbouring gaseous detectors. All detectors therefore incorporated water cooling in the end plates of the support structure, in close contact with the ‘hot’ readout electronics.

Although in principle the mechanical stability of the detector could be monitored using the data itself, two experiments (ALEPH, L3) also developed independent systems in which infra-red laser spots, mounted on

the inside of the outer tracking chamber, illuminated the silicon sensors at regular intervals. These devices turned out to be very useful and revealed many subtle effects related to thermal and humidity variations during the day-to-day operation [3].

2.2. The LEP vertex detectors

The ALEPH and DELPHI collaborations decided very early on (the 1982 letters of intent) to adopt the then novel silicon vertex detectors in the baseline design of their experiments. After several years of R&D, prototype modules were operated during the first data taking in 1989. In contrast, the OPAL and L3 collaborations decided much later to incorporate such detectors, benefiting from the space liberated by the reduction in the beam-pipe radius in 1991. For the second phase of LEP, motivated by the desire to maximise the potential for the detection of the Higgs particle via its characteristic decay into a pair of b quarks, many of the experiments decided to increase the solid angle coverage of their vertex detectors. The doubling in length of the original LEP1 detectors corresponded to a $\sim 30\%$ gain in statistics for the Higgs search. The layout of the four LEP2 versions of the detectors is shown in Fig. 3 and their characteristics are summarised in Table 1.

The ALEPH vertex detector [4] was first installed in 1989 and completed by 1991. In 1995, the detector was upgraded by doubling its length, removing the z -side electronics from the sensitive region, and adopting

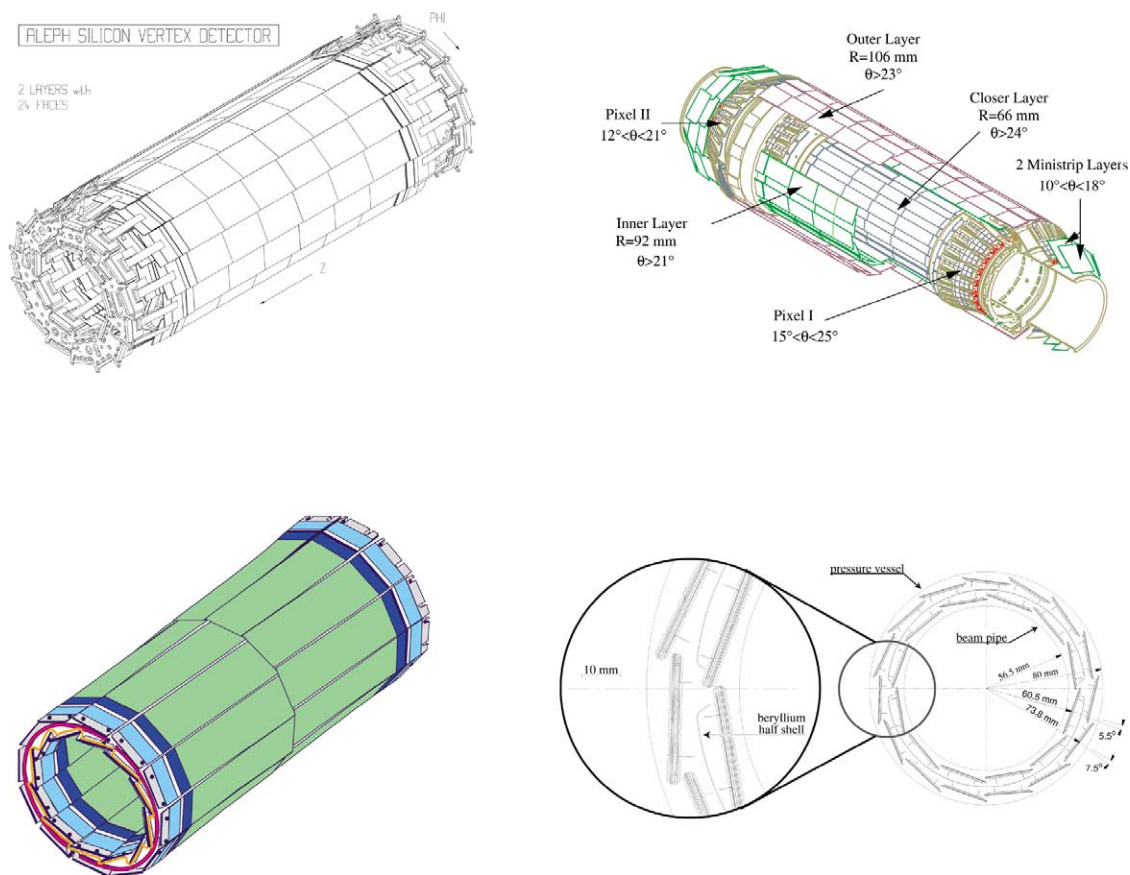


Figure 3. Layouts of the LEP2 vertex detectors. The ALEPH VDET II (top left), the DELPHI Silicon Tracker (top right), the SMD of L3 (bottom left) and the μ VTX3 of OPAL (bottom right).

Table 1. Characteristics of the LEP2 vertex detectors.

	ALEPH	DELPHI	L3	OPAL
Layers	2	3	2	2
Radii [cm]	6.3, 11.0	6.6, 9.2, 10.6	6.4, 7.9	6.1, 7.4
Modules/layer	9, 15	24, 20, 24	12	12, 15
Sensors/face	6	4, 8	4	5
Face length [cm]	40	28, 48	28	30
Max $ \cos \theta $	0.88, 0.95	0.91, 0.93	0.83, 0.93	0.89, 0.93
Overlaps [%]	5	12–15	12, 0	0
Channels	95k	150k	73k	65k
Readout chip	MX7-RH	MX6,TRIPLEX	SVX-H3	MX7,MX7-RH
AC coupling	capacitor chip	integrated	capacitor chip	integrated
Sensor type	double-sided	double + single	double-sided	single-sided
z readout	polyamide fanout	double-metal	kapton fanout	glass
Readout pitch [μm]	ϕ :50, z :100	ϕ :50, z :44–176	ϕ :50, z :150, 200	ϕ :50, z :100
Material [% of X_0]	1.5	3.1	1.2	1.5
Support structure	hollow carbon fibre	carbon honeycomb	carbon honeycomb	beryllium
Cooling	water + air	water	water	water + N_2
Stability monitor	laser	–	laser	–
Sensitive area [m^2]	0.96	$1.37 + 0.41$ (VFT)	0.52	0.53

radiation-hard readout electronics. ALEPH was the first experiment to use double-sided sensors with readout strips on both sides of the same silicon sensor. The readout was performed with the MX7 front-end chip, AC-coupled to the silicon via diode-protected capacitor chips located on the hybrids at both ends of the faces. The z strips were rerouted to the end of the face using a thin polyamide fanout glued on top of the sensors and wire-bonded to the strips.

The DELPHI silicon tracker [5], first installed in 1989, was continuously upgraded, evolving from two to three layers and single-sided to double-sided. The final LEP2 configuration consisted of a three layer microstrip vertex detector in the barrel, and a Very Forward Tracker (VFT) of two layers of ministrip and pixel sensors in the endcaps. The two inner layers were built from double-sided sensors, while the outer layer used back-to-back single-sided detectors. The DELPHI sensors featured an additional double-metal layer, which allowed the AC coupling and routing of the z -side strips to the end of the detector to be directly incorporated in the silicon. The readout pitch, on the z side, varied with polar angle.

The DELPHI endcaps consisted of 152 macro-pixel sensors and 48 mini-strip modules arranged in the form of cones. The pixels had dimensions of $330 \mu\text{m} \times 330 \mu\text{m}$ and the readout buses were integrated into the sensors again via a double-metal layer. The readout electronics (SP8) were bump-bonded to the sensors using an IBM process. To reduce the data size, a sparse data scan scheme was implemented in which noisy pixels, identified in regular calibration runs, were masked. The DELPHI experiment was the first collider experiment to use such pixel sensors for tracking.

The L3 vertex detector [6] proposed in 1991 and installed in 1993, was built from two radial layers of ALEPH like double-sided sensors. No further upgrade was performed. In order to facilitate pattern recognition, the L3 design incorporated a unique feature, in which the faces of the outer layer were tilted

by 2 degrees with respect to the beam direction. The readout pitch on the z side changed from 150 μm to 200 μm for tracks at large incident angles.

The OPAL vertex detector [7], proposed in early 1990 and very quickly operational in 1991 initially consisted of two layers of single-sided sensors. In 1993, the detector was upgraded to both $r\phi$ and z measurements using back-to-back single-sided detectors. The length of the detector was subsequently increased in 1995. A beryllium mechanical support, rather than carbon fibre, was utilised. OPAL chose a 200 μm thin glass substrate with gold traces to route the z strip signals to the readout electronics.

2.3. Detector performance

The performance of the LEP vertex detectors is summarised in Table 2. The signal-to-noise ratios obtained in the detectors all had a most probable value greater than 10, with values usually larger than 20. This allowed low thresholds to be applied, yielding a high efficiency for the detection of a traversing charged particle. The overall efficiency of the detectors was therefore determined by failure of the individual sensors, with efficiencies in excess of 95% achieved. For the DELPHI VFT pixel and ministrip detectors, efficiencies of >96% were obtained after excluding failing sensors (10% of the pixels and 6% of the ministrips failed after three years of running). Random hits due to noise were kept below one ppm.

As shown in Fig. 4, the point resolutions, measured using the residuals of tracks traversing at least three layers (for example in the overlap regions), were between 8 and 10 μm in the plane transverse to the beam ($r\phi$) and between 11 and 20 μm along the beam direction (z) for particles at normal incidence. The $r\phi$ resolution improves slightly at large polar angles due to the increased energy deposition. The z resolution is observed to increase with polar angle due to the larger spread of the signal with increased incident angle and also the higher probability of producing energetic delta rays. This increase can be partially reduced by increasing the z readout pitch at larger $\cos\theta$ as done by DELPHI and to some extent L3.

In terms of the impact parameter resolution previously discussed, the intrinsic term can be readily determined (see Fig. 5) by measuring the miss distance between high momentum muons in $Z \rightarrow \mu^+\mu^-$ events; values obtained are 20–30 μm in $r\phi$ and 25–130 μm in z . The multiple scattering term (see Fig. 5) also can be determined by a fit of the measured impact parameter as a function of particle momenta and polar angle; values obtained are 70–100 $\mu\text{m GeV}/c$. In terms of vertexing in b events, typical decay length resolutions of $\sim 250 \mu\text{m}$ are obtained, an order of magnitude smaller than the average b decay length.

Table 2. Summary of the performances of the LEP2 vertex detectors [8].

	ALEPH	DELPHI	L3	OPAL
Signal-to-noise ($r\phi$)	31	10–28	18	24/29
Signal-to-noise (z)	18	10–28	18	20/24
Point resolution ($r\phi$) [μm]	8	8	8	8–10
Point resolution at 90° (z) [μm]	12	11	20	10–12
i.p. resolution ($r\phi$) [μm]	34 ^a	25	30	18
i.p. resolution (z) [μm]	34 ^a	34	130	24
Multiple scattering term ^b [$\mu\text{m GeV}/c$]	70	70	80	100

^a ALEPH only quotes the resolution for a three-dimensional impact parameter (i.p.).

^b Estimated from fits with one constant term and one proportional to $(p \sin^{3/2} \theta)^{-1}$.

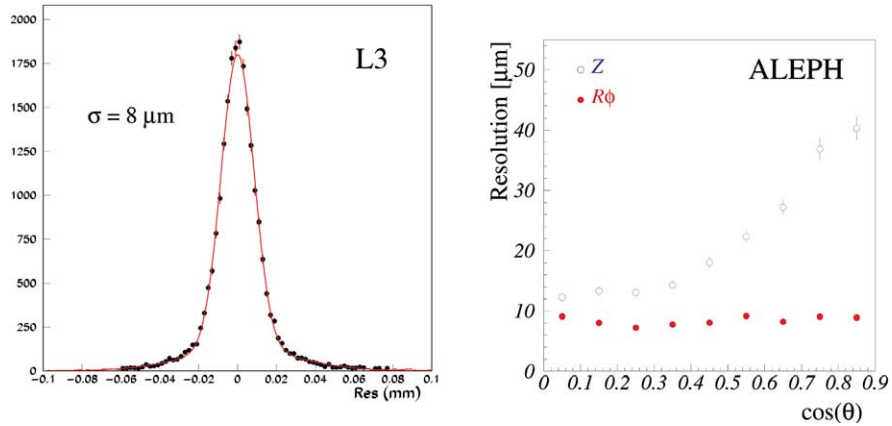


Figure 4. Left: the $r\phi$ spatial resolution of the L3 SMD; right: the $r\phi$ and z spatial resolutions of the ALEPH VDET II as a function of polar angle.

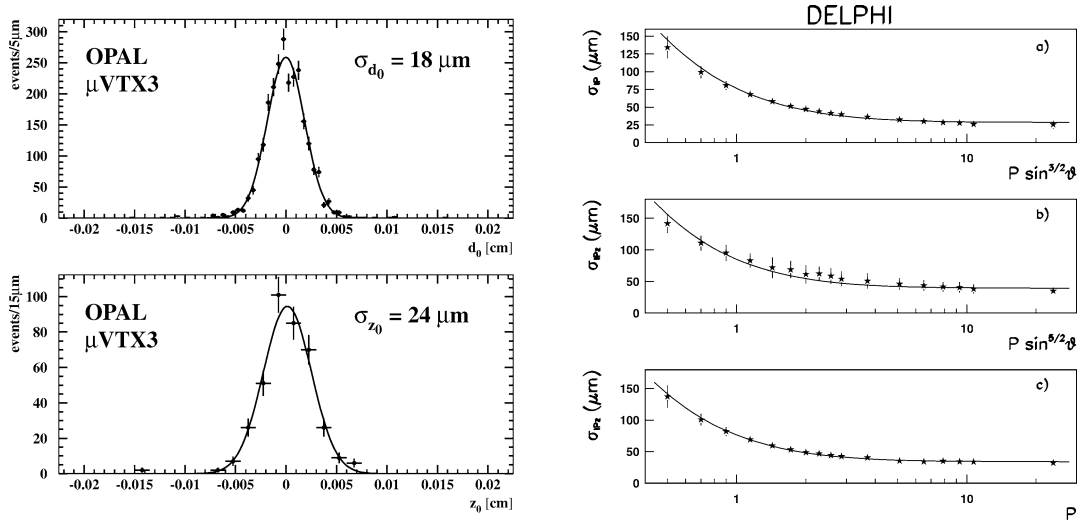


Figure 5. Left: the geometric contribution to the impact parameter resolution of the OPAL detector, measured using $e^+e^- \rightarrow \ell^+\ell^-$ events, in $r\phi$ (top) and z (bottom). Right: the impact parameter resolution as a function of particle momentum and polar angle in DELPHI for (a) $r\phi$; (b) z all incident angles; and (c) z normal incidence.

3. Direct lifetime measurements at LEP

Direct lifetime measurements (based on topology rather than decay width) have been performed at LEP for the most common weakly-decaying b-hadrons species, as well as for the τ lepton. All the lifetime analyses rely on the vertex detector data to measure the decay products and to reconstruct an estimate of the production point. The latter can be obtained in each $Z \rightarrow b\bar{b}$ event using tracks from fragmentation (or decay of strong b-hadron resonances) produced at the interaction vertex in conjunction with the pair of weakly decaying b hadrons. However, in $Z \rightarrow \tau^+\tau^-$ events, all charged tracks are produced at the decay points of the two τ leptons, so in this case the interaction vertex cannot be reconstructed on an event-by-event basis. The only available information on the τ production point is the position and size of the luminous region, determined from hadronic Z decays averaged over small chunks of consecutive events. The precision reached on the position of this beam spot is typically of order 10 μm , and its RMS dimensions are approximately 7 mm in the beam direction, and 150 μm (5 μm) horizontally (vertically) in the transverse plane.

As sketched in Fig. 6, lifetimes can be extracted in two different ways. Firstly, the decay vertex can be reconstructed from the decay products; together with the production vertex, this yields a decay length L . If an estimate of the momentum p is available, then the proper flight time can be obtained as $L \times m/p$, where m is the mass of the decaying particle (note that this can also be done using the projections of L and p on the transverse plane). Secondly, the average proper time can be obtained from the distribution of the impact parameter of one of the decay products with respect to the production vertex; in the limit of a highly relativistic decaying particle, this impact parameter becomes independent of p , since the increase in decay length due to the relativistic boost is compensated by the decrease of the average decay angle in the laboratory. The average τ lifetime and, consequently, the mean impact parameter from τ products are approximately 6 times smaller than in the case of b hadrons; hence τ lifetime measurements are in principle more difficult and rely more on the good resolution of the vertex detector. However, it is interesting to note that, at the Z, the average τ decay length is comparable to that of b hadrons, because the smaller lifetime is compensated by a larger boost.

3.1. τ lifetime measurements

Several methods have been used to extract the mean τ lifetime [9]. The decay length method, in which the decay point of three-prong τ decays is reconstructed, makes use of the beam spot information. Because of the large longitudinal size of the beam spot, the decay length is effectively measured in the transverse plane before being converted into three dimensions using an estimate of the polar angle of the τ direction. The dominant source of uncertainty is the statistical uncertainty related to the natural width of the exponential distribution. This is a very powerful technique, however it can only be applied to about $\sim 15\%$ of all τ decays.

For a one-prong τ decay, i.e., a decay to a single charged track, it is not possible to reconstruct, on an individual basis, the τ decay point or its direction. However, different techniques have been developed to extract the lifetime. The simplest consists of measuring the distribution of the signed impact parameter distribution (in the transverse plane) of the single prong with respect to the interaction point (the sign is negative if the track appears to travel backward relative to the τ direction determined from the event thrust axis), the dependence of which is determined from Monte Carlo simulation (roughly proportional to the τ lifetime). In the impact-parameter difference (IPD) technique, applied to events with both τ 's decaying to a single charged track, the lifetime is extracted from the correlation between the difference of the two track impact parameters and the difference of their azimuthal angles. Other techniques measure the distribution of the impact-parameter sum (IPS), the lifetime dependence of which is parametrised from Monte Carlo simulations. While the uncertainty on the production point enters twice in the IPD method, it nearly cancels in the IPS method. On the other hand, the IPD and IPS method are insensitive and sensitive, respectively, to the assumed impact parameter resolution. Finally a real three-dimensional impact parameter method was developed, the most sensitive for one-prong decays, to make use of all the kinematical information (in $\tau \rightarrow$ hadron decays), as well as the impact parameter information from the rz view of the vertex detector.

An example of τ decay length distribution is shown in Fig. 7. The world average of all τ lifetime measurements is (290.6 ± 1.1) fs [11], completely dominated by LEP, with a combined total uncertainty that has decreased by a factor 8 since the start of LEP [12]. As discussed in the contribution by Rougé and Tanaka [13], this result and its high precision are very important ingredients to test the universality of the couplings of the different leptons to the W gauge boson.

3.2. b-hadron lifetime measurements

In the spectator model of hadron decays, a heavy quark Q is considered to decay without interacting with the other light quark(s) in the hadron, and hence all hadrons containing a particular heavy quark are predicted to have equal lifetimes. This model fails dramatically in the charm sector, where large differences are observed: $5\tau(\Lambda_c) \sim 2.5\tau(D^0) \sim 2.5\tau(D_s^+) \sim \tau(D^+)$. This can be explained if additional effects are taken into account, such as final state interference, annihilation and W-exchange processes, as well as helicity suppression. A systematic QCD-based theoretical treatment has been developed where the

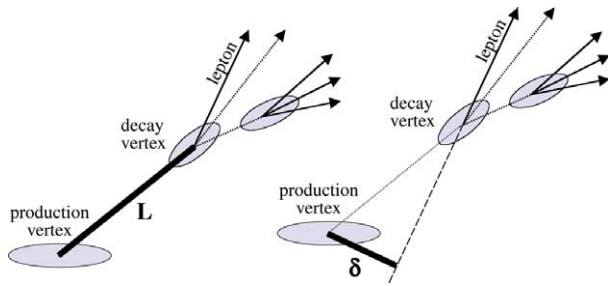


Figure 6. Definitions of the decay length L and impact parameter δ in case of a semi-leptonic b-hadron decay with the same topology as in Fig. 1 (not to scale).

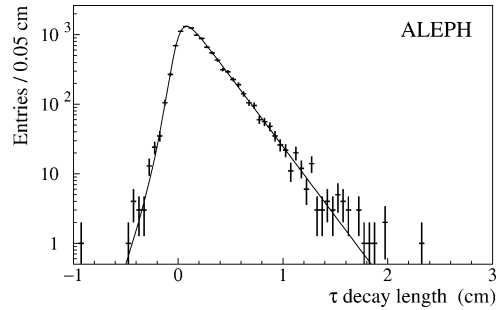


Figure 7. Decay length distribution for three-prong τ decays in ALEPH [10].

decay rates of heavy hadrons are expressed as expansions in powers of $1/m_Q$. In this approach, lifetime differences only arise at order $1/m_Q^2$ between baryons and mesons, whereas differences between mesons emerge at order $1/m_Q^3$. This heavy quark expansion (HQE) may be questionable when applied to the charm sector (despite its reasonable success), but is expected to be more reliable for b-hadron lifetime differences, because of the larger b-quark mass. The predicted hierarchy $\tau(\Lambda_b) < \tau(B^0) \simeq \tau(B_s^0) < \tau(B^+)$ is similar to that observed in the charm sector, but with significantly smaller differences. An exception is the B_c^+ meson, where both quarks can decay, resulting in a much shorter lifetime. Recent theoretical predictions, based on next-to-leading order QCD calculations and lattice determination of hadronic matrix elements, are $\tau(B^+)/\tau(B^0) = 1.06 \pm 0.02$, $\tau(B_s^0)/\tau(B^0) = 1.00 \pm 0.01$, and $\tau(\Lambda_b)/\tau(B^0) = 0.90 \pm 0.05$ [14]. Measurements of the individual lifetimes at the percent level are required to test these predictions.

Before LEP, only the inclusive b-hadron lifetime had been measured, which corresponds to the average of all individual b-hadron lifetimes weighted by their relative abundance in the selected sample (approximately 40% B^+ , 40% B^0 , 10% B_s^0 and 10% b baryons). Such measurements [15] have been repeated at LEP with much improved precision (now limited by systematics), based on the impact parameter of leptons selected with high momentum (due to the hard b fragmentation) and high transverse momentum (due to the large b mass), and the decay length obtained from secondary vertexes reconstructed in an inclusive manner. Examples of these two different techniques are shown in Fig. 8. The current world average of the inclusive b-hadron lifetime is (1.564 ± 0.014) ps [18], again completely dominated by the LEP measurements. This can be compared with the average available before LEP, (1.18 ± 0.11) ps [12], which was almost an order of magnitude less precise and appears now to have been $\sim 3.5\sigma$ low.

Lifetimes for individual b-hadron species have usually been extracted from decay length and momentum measurements [15]. In principle, the ideal method is to fully reconstruct specific decays: this gives the best vertex resolution, momentum estimate and separation between the b-hadron species. However, the statistics available at LEP are too low for this method to compete with more inclusive techniques where, for example, a fully-reconstructed charmed hadron X_c is associated with a nearby lepton of appropriate charge (in this case, the b-hadron momentum is estimated from that of the $X_c\ell$ combination, with a correction for the missing particles from Monte Carlo simulation).

Such techniques based on $D^{(*)}\ell$ correlations have been used successfully to extract the B^+ and B^0 lifetimes (since $B^+ \rightarrow \bar{D}^0\ell^+\nu$ and $B^0 \rightarrow D^{*-}\ell^+\nu$), in spite of the relatively important cross-feed induced by the decays of D^* and higher resonances. An alternative method to extract $\tau(B^+)$, $\tau(B^0)$ and their ratio is to use inclusive secondary vertexes and separate B^+ and B^0 mesons by counting the total charge of the tracks from the decay vertex or applying more elaborate neural network techniques (see Fig. 9). For the B^0 lifetime, $B^0 \rightarrow D^{*-}\ell^+\nu$ events have also been used, where the D^{*-} has been identified inclusively by the slow pion from the $D^{*-} \rightarrow \bar{D}^0\pi^-$ decay. For the B_s^0 lifetime, the most powerful analyses are those based on $D_s^\pm\ell^\mp$ correlations (see Fig. 1), although more inclusive samples of D_s^\pm mesons have also been used.

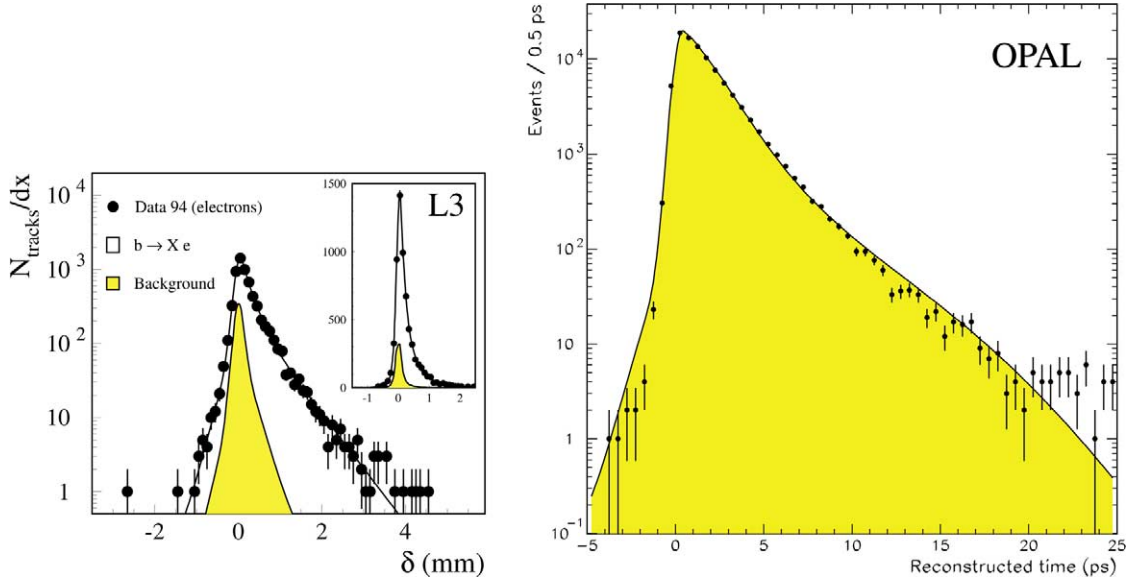


Figure 8. Left: lepton impact parameter distributions from L3 [16]; right: inclusive b-hadron proper-time distribution measured by OPAL [17].

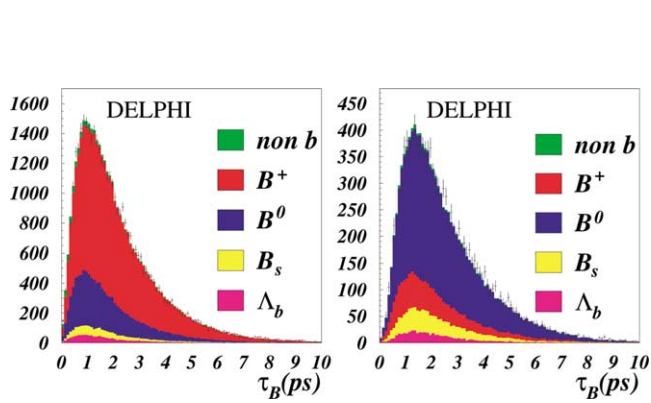


Figure 9. Proper time distributions obtained by DELPHI from samples of inclusive secondary vertexes, enriched in B^+ (left) and B^0 (right); the sample compositions, shown as filled histograms, are obtained from Monte Carlo simulation [19].

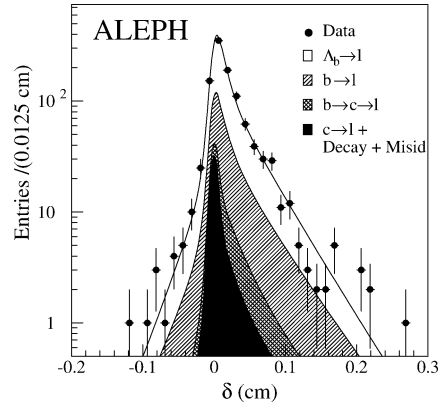


Figure 10. Lepton impact parameter distribution of Λ_c^- candidates from ALEPH [20].

Several techniques have been developed for the b baryons, all based on semileptonic decays. An average b-baryon lifetime can be obtained from $\Lambda \ell^-$ or $p \ell^-$ correlations, where the lepton arises from the decay of the b baryon, and the Λ or proton from the subsequent decay of the charmed baryon; hence the identified particles are not expected to come from a common vertex, and an impact parameter method is used, as illustrated in Fig. 10. The Λ_b lifetime can be obtained from decay length measurements with $\Lambda_c^+ \ell^-$ correlations, where the Λ_c^+ is either fully reconstructed or partially reconstructed in the $\Lambda_c^+ \rightarrow \Lambda \ell^+ X$ mode. Finally the average strange b-baryon (Ξ_b) lifetime has been measured from the lepton impact parameter distribution in events with $\Xi^- \ell^-$ combinations.

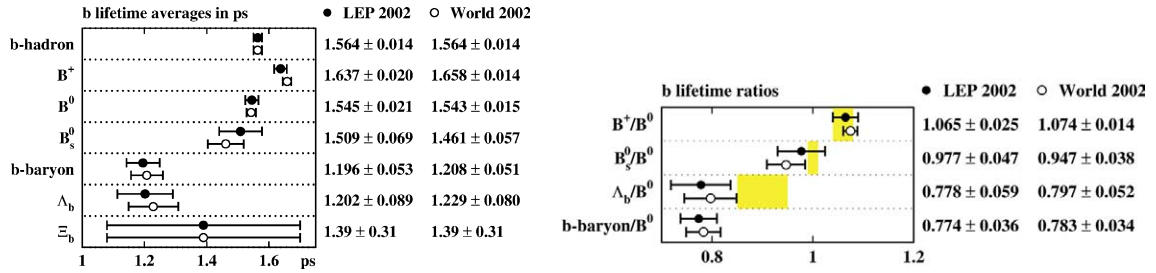


Figure 11. Summary of b-lifetime averages [18], including preliminary measurements as of Winter 2002. Decay width differences in the neutral B meson systems have not been observed, and have been assumed to be zero. The shaded areas represent the theoretical predictions of [14].

The different b-hadron lifetime results obtained by LEP are summarised and compared with the world averages in Fig. 11. In all cases, the precision achieved is largely due to the LEP measurements. Only this year have the combined non-LEP measurements of the B^+ and B^0 lifetimes reached a precision similar to the LEP averages, thanks to the large statistics available at the asymmetric B factories running at the $\Upsilon(4S)$. As also shown in Fig. 11, the theoretical predictions for the lifetime ratios are in reasonable agreement with the experimental measurements.

4. Conclusion

The successful and reliable operation of microstrip and pixel vertex detectors during the ten years of LEP's operation, has clearly demonstrated the coming of age of silicon detector technology. A plethora of physics results, relying on their precise tracking capabilities near to the interaction point, have been published by the LEP collaborations. In particular, the measurements of inclusive and exclusive particle lifetimes, have provided precise measurement of fundamental physics parameters and tested our understanding of quark dynamics.

Acknowledgements. L. Di Ciaccio, H.-G. Moser, C. Shepherd-Themistocleus are acknowledged for providing the b-hadron lifetime averages.

References

- [1] E. Fernandez, et al., MAC Collaboration, Phys. Rev. Lett. 51 (1983) 1022; N.S. Lockyer, MARKII Collaboration, Phys. Rev. Lett. 51 (1983) 1316.
- [2] P. Kluit, A. Stocchi, Heavy quarks and the CKM matrix, C. R. Physique 3 (2002) 1203.
- [3] G. Sguazzoni, et al., Nucl. Phys. B 78 (1999) 301.
- [4] D. Creanza, et al., Nucl. Phys. B 61 (1998) 201.
- [5] P. Chochula, et al., Nucl. Instrum. Methods A 412 (1998) 304.
- [6] M. Accari, et al., Nucl. Instrum. Methods A 351 (1994) 300.
- [7] S. Anderson, et al., Nucl. Instrum. Methods A 403 (1998) 326.
- [8] K. Österberg, Nucl. Instrum. Methods A 435 (1999) 1.
- [9] S.R. Wasserbaech, hep-ex/9811037.
- [10] R. Barate, et al., ALEPH Collaboration, Phys. Lett. B 414 (1997) 362.
- [11] D.E. Groom, et al., Particle Data Group, Eur. Phys. J. C 15 (2000) 1.
- [12] J.J. Hernández, et al., Particle Data Group, Phys. Lett. B 239 (1990) 1.
- [13] A. Rougé, R. Tanaka, C. R. Physique 3 (2002) 1165.
- [14] E. Franco, V. Lubicz, F. Mescia, C. Tarantino, hep-ph/0203089.
- [15] ALEPH, CDF, DELPHI, L3, OPAL, SLD Collaboration, CERN-EP/2001-050, and references therein.
- [16] M. Acciarri, L3 Collaboration, Phys. Lett. B 416 (1998) 220.
- [17] K. Ackerstaff, et al., OPAL Collaboration, Z. Phys. C 73 (1997) 397.
- [18] b-hadron lifetime working group, <http://www.cern.ch/LEPBOSC/lifetimes/>.
- [19] DELPHI Collaboration, DELPHI 2001-051 CONF 479, Contribution #300 to Int. Europhysics Conf. on High Energy Physics, Budapest, Hungary, 2001.
- [20] D. Buskulic, et al., ALEPH Collaboration, Eur. Phys. J. C 2 (1998) 197.